

Post-synthetic preparation of Sn-, Ti- and Zr-beta: a facile route to water tolerant, highly active Lewis acidic zeolites†

Cite this: *Dalton Trans.*, 2014, **43**, 4514

Patrick Wolf, Ceri Hammond, Sabrina Conrad and Ivo Hermans*

Received 22nd October 2013,
Accepted 3rd January 2014

DOI: 10.1039/c3dt52972j

www.rsc.org/dalton

A two-step procedure for the post-synthetic preparation of Lewis acidic Sn-, Zr- and Ti-zeolite β is reported. Dealumination of a commercially available Al- β zeolite leads to the formation of highly siliceous material containing silanol nests, which can be filled in a second step *via* the solid-state ion-exchange or impregnation of an appropriate metal precursor. Spectroscopic studies indicate that each metal is subsequently coordinated within the zeolite framework, and that little or no bulk oxides are formed – despite the high metal loadings. The synthesised catalysts demonstrate excellent activity for the isomerisation of glyceraldehyde to dihydroxyacetone, a key model reaction for the upgrading of bio-renewable feedstocks, and the epoxidation of bulky olefins.

Introduction

In recent times, water tolerant, heterogeneous Lewis acids have found widespread applicability for a number of liquid phase oxidation and isomerization reactions.¹ Most notable amongst this class of materials are Lewis acid-containing zeolites. Unlike traditional stoichiometric and/or homogeneous Lewis acids, *e.g.* Zn^{II} and Al^{III}, these heterogeneous materials avoid the (co)-production of copious amounts of inorganic and/or toxic waste, and avoid a number of downstream handling problems *viz.* separation. Moreover, the encapsulation of the Lewis acid inside a water-resistant, hydrophobic framework (as found for highly siliceous zeolites) prevents the hydrolysis and subsequent deactivation of the Lewis acid, and thereby allows these promising materials to be utilised for aqueous phase oxidation and isomerisation reactions.²

Of particular interest is Sn^{IV}-containing zeolite β (Sn- β). This catalyst has demonstrated an exceptional ability to activate carbonyl-containing molecules, and has thus found widespread applicability as a promising catalyst for the Baeyer–Villiger oxidation of ketones to lactones using H₂O₂,³ and the upgrading of bio-renewable platform molecules, such as glucose.⁴ Indeed, Sn- β -catalysed isomerization of glucose to fructose is the first step in perhaps the most promising route towards the upgrading of glucose (and eventually cellulose) to

various fuels and chemicals.^{5,6} In addition to the promising catalytic results obtained with Sn- β , exciting results have also been obtained by other Lewis acidic zeolites. For example, Zr^{IV}-containing β -zeolite has recently been shown to be a promising catalyst for the production of γ -valerolactone from bio-renewable furfural,⁷ and the cascade transformation of citral to \pm -menthol.⁸ Zr^{IV}-containing silicates have recently also shown promising activity as CO₂ adsorbents.⁹ Furthermore, Ti^{IV} is also the critical component of many highly active and selective oxidation catalysts, such as TS-1, Ti- β and Ti-MWW zeolites.¹⁰

Despite increasing academic and industrial interest in this class of catalyst, some significant practical hurdles remain that currently curtail industrial implementation. Amongst these, the lengthy and complicated hydrothermal synthesis procedure, the low amount of active metal typically incorporated per kilogram of the final catalyst, and the large crystallite sizes remain the most prohibitive. Therefore alternative methods which do not suffer from these drawbacks are of great interest.¹¹

Recently, some of us reported a convenient post-synthetic route for the incorporation of Sn^{IV} into the framework of zeolite β .¹² In brief, the desired Lewis acid was incorporated into the vacant tetrahedral (T)-sites of a pre-dealuminated framework by solid-state ion-exchange. Not only does this approach avoid the long synthesis times associated with conventional hydrothermal synthesis routes, but also it allows for the synthesis of a material with significantly smaller crystallite sizes, higher metal content, and more favourable catalytic properties. Indeed, the catalytic productivity of post-synthetically prepared Sn- β was found to be five to ten times larger than previously reported for the Baeyer–Villiger oxidation of

ETH Zurich, Department of Chemistry and Applied Biosciences, Wolfgang-Pauli-Strasse 10, 8093 Zurich, Switzerland. E-mail: hermans@chem.ethz.ch;
Fax: +41 44 6331514; Tel: +41 44 6334258

† Electronic supplementary information (ESI) available. See DOI: 10.1039/c3dt52972j

cyclohexanone with H_2O_2 , and the conversion of dihydroxyacetone into ethyl lactate. In this publication, we extend our post-synthetic route for the preparation of Sn- β to other Lewis acids, such as Zr^{IV} and Ti^{IV} , with the aim of developing more convenient synthetic routes for other promising Lewis acidic zeolites.

Results and discussion

Dealumination of H-zeolite β

To create the necessary vacant framework sites for the incorporation of the desired Lewis acidic species, a parent aluminosilicate zeolite β ($\text{SiO}_2/\text{Al}_2\text{O}_3$ molar ratio = 25 (3.1 wt% Al), H-form) was first dealuminated by an established literature procedure,¹³ by treatment with concentrated HNO_3 (13 M, 100 °C, 20 h). Unlike steaming, dealumination by HNO_3 ensures that little or no extra-framework Al^{III} , a strong Lewis acid, remains in the material, thereby ensuring a clean, naked framework into which other Lewis acid centres can be incorporated. ICP-OES analysis demonstrated that Al^{III} was easily removed from the material (Table 1), with no negative changes to the structural integrity of the zeolite *cf.* pore volume, surface area and XRD patterns (Fig. 1).

Transmission FT-IR spectroscopy of the parent H-zeolite β demonstrates that the untreated material contains both Brønsted acid sites (charge compensatory protons occupying the cation-exchange sites, Si-O(H)-Al, 3610 cm^{-1}) and isolated silanol groups (-SiOH, 3740 cm^{-1}) at the external surface(s) of the zeolite (Fig. 2). Following HNO_3 treatment, the Si-O(H)-Al stretch is completely removed from the FT-IR spectrum, further indicating the complete removal of framework Al^{III} and the corresponding loss of cation-exchange sites. Along with an increased signal associated with isolated silanol species (3740 cm^{-1}), the dealuminated material also contains a broad absorbance at $\pm 3550 \text{ cm}^{-1}$. This broad feature is indicative of a network of hydrogen bonding within the structure of the zeolite, and has been attributed to the presence of silanol nests, $(\text{SiOH})_4$.¹³

Synthesis of Sn-, Zr- and Ti-zeolite β

Our previous work in this area has demonstrated that the formation of silanol nests is a pre-requisite for incorporating

Table 1 Physicochemical properties of Lewis acidic zeolites

Entry	Catalyst	Treatment ^a	S_{BET}^b ($\text{m}^2 \text{g}^{-1}$)	Metal loading (wt%)
1	H- β	—	600	3.1
2	deAl- β	H^+	620	<0.1
3	Sn- β	H^+ /SSIE (Sn(II) acetate)	600	10.1
4	Zr- β	H^+ /SSIE (Zr(IV) ethoxide)	580	7.7
5	Ti- β	H^+ /IMP (Ti(IV) ethoxide)	610	4.0

^a H^+ = acidic pre-treatment (HNO_3 , 13 M, 100 °C, 20 h); SSIE = solid-state ion-exchange reaction; IMP = impregnation. ^b Brunauer-Emmett-Teller surface area calculated by N_2 physisorption.

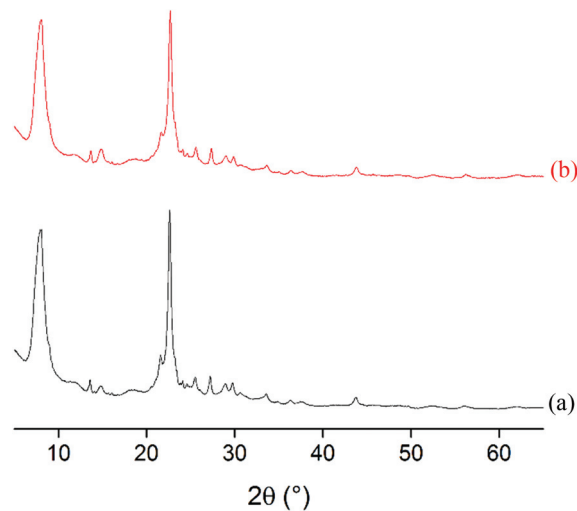


Fig. 1 XRD patterns for (a) untreated H-zeolite β ($\text{SiO}_2/\text{Al}_2\text{O}_3 = 25$) and (b) HNO_3 -treated zeolite β ($\text{SiO}_2/\text{Al}_2\text{O}_3 \geq 1000$).

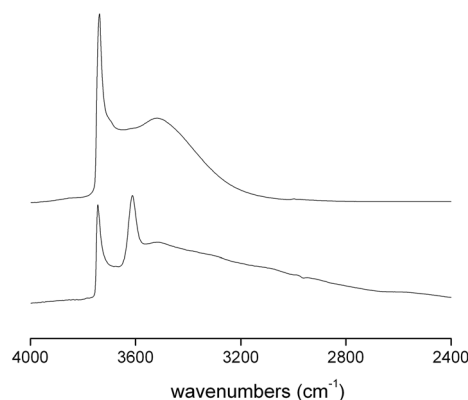


Fig. 2 FT-IR spectra for (bottom) untreated H-zeolite β ($\text{SiO}_2/\text{Al}_2\text{O}_3 = 25$) and (b) HNO_3 -treated zeolite β ($\text{SiO}_2/\text{Al}_2\text{O}_3 \geq 1000$). These data were partly published previously in *Angew. Chem., Int. Ed.*, 2012, **51**, 11736.

Lewis acids or other transition metals into the framework of zeolite β . Having achieved this aim, we subsequently turned our focus to the incorporation of Sn^{IV} , Zr^{IV} and Ti^{IV} . In order to prepare these samples, two preparation procedures were employed. For Sn- and Zr- β , we employed a solid-state ion-exchange procedure, which involves the mechanical grinding of dealuminated zeolite β with an appropriate solid metal precursor (Sn(II) acetate and Zr(IV) ethoxide, respectively). For Ti- β , the absence of a suitable solid precursor forced us to employ an impregnation methodology, involving the wet impregnation of dealuminated zeolite β with an ethanolic solution of Ti(IV) ethoxide. The preparation of each as synthesised sample was completed by a high-temperature calcination procedure (550 °C, 3 h, flowing air) in order to remove the residual acetate/ethoxide species, and to ensure complete encapsulation of the Lewis acid into the vacant framework sites. We note that each sample was prepared to contain the same molar ratio (*i.e.* 0.84 mmol metal per g catalyst), but that for

simplicity each sample will be denoted by its total metal content, *i.e.* wt%. Therefore, Sn^{IV} zeolite β , containing 10.1 wt% Sn, will be denoted as 10Sn- β .

Characterisation of Sn-, Zr- and Ti-zeolite β

Unlike trivalent metals, *e.g.* Al^{III}, the coordination of tetra-valent metals into the zeolite framework, *e.g.* Sn^{IV}, does not give rise to a negatively charged framework or cation-exchange sites. Thus, other than the complete consumption of the silanol nests feature ($\pm 3550\text{ cm}^{-1}$),¹⁴ FT-IR spectroscopy provides very little information on these Lewis acidic zeolites. However, analysis of the Diffuse Reflectance spectra in the UV-Vis region (DRUV-Vis) provides a great deal of information on the nature of the as synthesised species. The spectrum obtained for 10Sn- β features a sharp maximum at *ca.* 216 nm, which is indicative of isolated, tetrahedral Sn^{IV} species in the zeolite framework. As can be observed (Fig. 3), the spectrum for 10Sn- β is significantly blue-shifted with respect to the bulk metal oxide, SnO₂. In contrast, the spectra obtained for 8Zr- β and 4Ti- β are somewhat broader and less defined than 10Sn- β . Originally, we presumed that the broad patterns indicated the formation of multiple metal species, *e.g.* isolated metal sites, dimers/oligomers and/or bulk metal oxides. Nevertheless, no indication of absorbance at $\pm 350\text{ nm}$ was observed for 4Ti- β , suggesting little or no presence of TiO₂ (nano)particles, and the observed UV-Vis spectrum is very similar to those reported by Mania *et al.*, Hereijgers *et al.*, and Blasco *et al.*, where isolated Ti^{IV} sites were found following detailed spectroscopic analysis.¹⁵ Similarly, despite the DRUV-Vis pattern of 8Zr- β being somewhat broader than that of 10Sn- β , no absorbances were found above $\pm 250\text{ nm}$. From this, we conclude that each catalyst contains (predominantly) isolated, tetrahedrally coordinated Lewis acids within the framework of the zeolite, and few (or no) bulk oxides. However, in the absence of *e.g.* XAS or STEM analysis, the complete absence of bulk oxides is not yet conclusive.

For further information on the Lewis acid speciation within each sample, we subsequently turned to *in situ* analysis of the

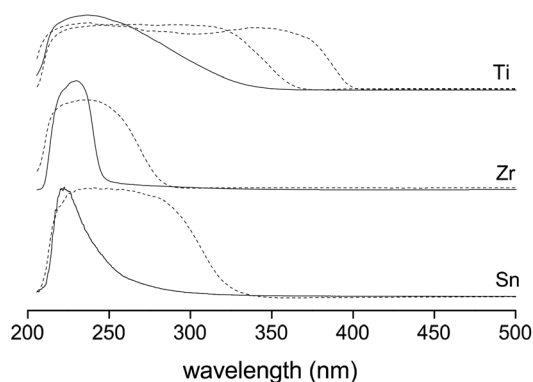


Fig. 3 DRUV-Vis spectra for (a) 10Sn- β (b) 8Zr- β and (c) 4Ti- β . Dashed lines overlaid with each spectrum are the DRUV-Vis spectrum obtained for the corresponding bulk metal oxide (SnO₂, ZrO₂ and TiO₂ (anatase and rutile)).

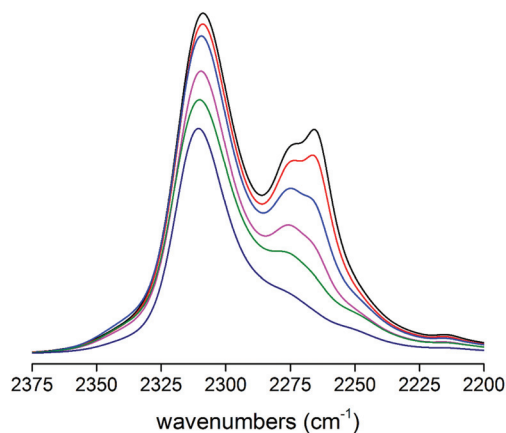


Fig. 4 *In situ* CD₃CN adsorption/desorption profile for 10Sn- β . CD₃CN was desorbed under static vacuum for various time periods (increasing from top to bottom), and all spectra are background-referenced against the dehydrated zeolite sample.

catalysts with CD₃CN absorption (*i.e.* probe molecule studies). It has previously been demonstrated¹⁶ that when coordinated within the zeolite framework, Lewis acidic centres dosed with CD₃CN give rise to an absorption in the FT-IR spectrum at $\pm 2310\text{ cm}^{-1}$. This feature has been attributed to the coordination of CD₃CN onto the isolated, framework-incorporated Lewis acidic centre (CD₃CN–Lewis acid), and is not observed for bulk metal oxides. The presence of this band at 2310 cm^{-1} thus provides information on the degree of Lewis acidity in a sample.

Fig. 4 presents the full adsorption/desorption spectrum for 10Sn- β . Following adsorption of CD₃CN, two major adsorption features are observed at ± 2270 and $\pm 2310\text{ cm}^{-1}$. The first feature is indicative of CD₃CN weakly physisorbed onto the sample. The second feature at 2310 cm^{-1} corresponds to CD₃CN coordinated onto the Sn^{IV} Lewis acid centre, and conclusively demonstrates that Sn^{IV} is isolated and present in the zeolite framework. It is noticeable that a shoulder at $\pm 2275\text{ cm}^{-1}$ is present on the physisorbed CD₃CN feature. This has previously been attributed to CD₃CN coordinated to a Brønsted acid site. Its presence in the adsorption spectrum for 10Sn- β is likely due to the residual silanol species that are present in the material; even at a loading of 10 wt%, only around 90% of the silanol nests have been fully occupied by Sn, and thus a small fraction of vacant silanol nests – imparting weak Brønsted acidity – remain. This fraction could also be somewhat larger if not all the metal is present in the framework. Following desorption under static vacuum for various time periods, it is clear that the weakly-bound physisorbed CD₃CN is first removed, followed by the CD₃CN species bound to the Brønsted acid sites. It is apparent that the strength of the CD₃CN–Lewis acid species is quite high, as full removal of these species was not observed even following 16 minutes of evacuation.

A similar analysis of 8Zr- β and 4Ti- β demonstrated that these samples also contain isolated Lewis acid sites (Fig. 5),

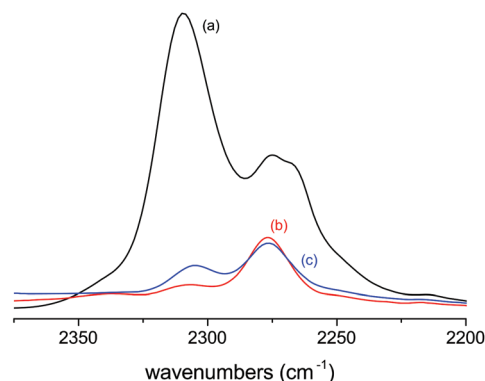


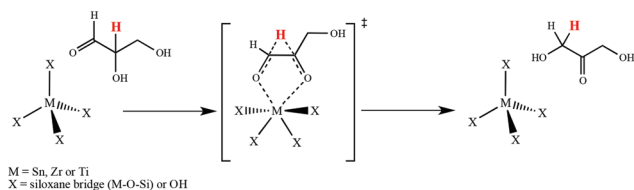
Fig. 5 CD_3CN adsorption/desorption profile for (a) 10Sn- β , (b) 8Zr- β , and (c) 4Ti- β following desorption for 4 minutes.

though the strength of these Lewis acidic centres appears to be somewhat lower than those found in 10Sn- β . For example, whilst evacuation of 10Sn- β for 4 minutes removed only weakly physisorbed CD_3CN , a similar treatment of 8Zr- β and 4Ti- β had a larger influence on the spectra (Fig. 5), with around one-half of the CD_3CN -Lewis acid absorption feature being lost. Whilst both 8Zr- β and 4Ti- β are apparently much less Lewis acidic than 10Sn- β , it is clear that the order of acidity follows the trend $\text{Sn} \gg \text{Zr} \cong \text{Ti}$.

Isomerisation of glyceraldehyde to dihydroxyacetone

Having established that each material contains isolated Lewis acid sites within the zeolite framework, we aimed to explore their relative catalytic activities for a series of reactions. As mentioned above, Lewis acid catalysed isomerisation has emerged as one of the most promising routes towards utilising cellulose-based feedstocks for the synthesis of chemicals and fuels.¹⁶ Although there remains much debate as to the structure of the active Lewis acid site (whether the Lewis acid is fully coordinated to the zeolite framework (closed) or partially hydrolysed (open)), this isomerisation is known to proceed *via* a 1,2-hydride shift, and is catalysed by the bidentate coordination of the reacting molecule (glucose) to the Lewis acidic centre (Scheme 1).¹⁷ The isomerisation of glyceraldehyde to dihydroxyacetone is therefore an ideal model reaction to investigate the catalytic activity of Lewis acidic zeolites for such isomerisation reactions.

However, despite its potential as a route towards utilising bio-renewable feedstocks, this isomerisation is a relatively slow reaction, and many consecutive and/or side products can also



Scheme 1 Schematic representation of the isomerisation of glyceraldehyde to dihydroxyacetone, catalysed by Lewis acidic zeolites.

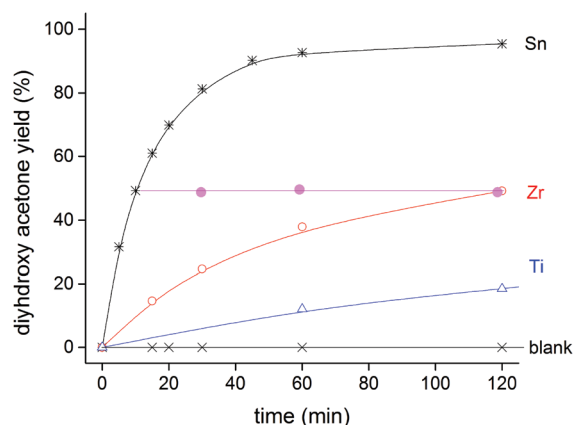


Fig. 6 Catalytic activity of (*) 10Sn- β , (o) 8Zr- β , (Δ) 4Ti- β , and (x) no catalyst for the isomerisation of glyceraldehyde to dihydroxyacetone. Catalytic activity of supernatant solution after removal of 10Sn- β at 10 minutes is also indicated (\bullet). Reaction conditions: 5 mL solution, 0.4 M glyceraldehyde in H_2O , 90 °C, substrate/metal ratio = 100.

be formed. Thus, as a simpler and more facile model reaction, we utilised the analogous 1,2-hydride shift reaction involving isomerisation of glyceraldehyde to dihydroxyacetone as a means of exploring the relative reactivities of the synthesised catalysts. Nevertheless, in order to be fully representative of the isomerisation of glucose to fructose, the isomerisation of glyceraldehyde to dihydroxyacetone was performed in the aqueous phase.

A recent theoretical analysis has proposed that for this specific aqueous phase reaction, the order of reactivity for these catalysts should be: $\text{Sn} \gg \text{Zr} > \text{Ti}$.¹⁸ As can be seen (Fig. 6), all synthesised solids demonstrate catalytic activity for this reaction, confirming their successful synthesis by post-synthetic methods. Furthermore, and in excellent agreement with the theoretical calculations, our preliminary experiments demonstrate that 10Sn- β displays exceptional activity for the isomerisation of glyceraldehyde ($R^{\text{init}} = 15.8 \text{ mmol min}^{-1}$), and that 8Zr- β and 4Ti- β are around one order of magnitude less active (2.8 and 1.2 mmol min^{-1} , respectively). In all cases, dihydroxyacetone was the major product obtained at >95% selectivity, though trace quantities of pyruvic aldehyde were observed above 95% conversion.

It is clear that the order of reactivity is in agreement with both the apparent Lewis acid strength as obtained from *in situ* CD_3CN adsorption studies and the order of reactivity proposed by theoretical studies. To further examine this link between experiment and theory, we explored the catalytic activity of 10Sn- β over a temperature range of 50–100 °C (ESI Fig. S1†), and found that the obtained Arrhenius temperature dependence (16.6 kcal mol^{-1}) for 10Sn- β agrees to an excellent degree with the theoretical predictions of Assary and Curtiss (15.4 kcal mol^{-1} ; Fig. 7).¹⁸

Epoxidation of cyclooctene with H_2O_2

Despite the activity of all the catalysts for the isomerisation of glyceraldehyde to dihydroxyacetone, the low activity of 4Ti- β

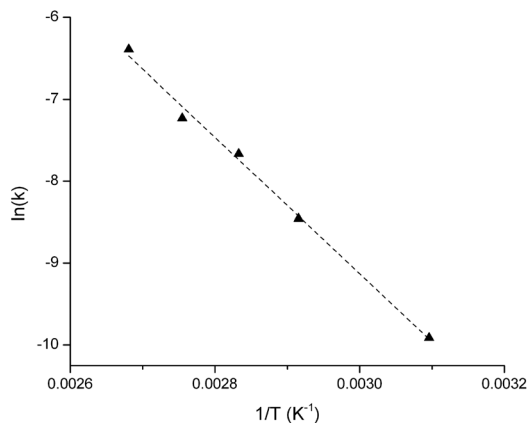


Fig. 7 Arrhenius plot for 10Sn- β for the isomerisation of glyceraldehyde to dihydroxyacetone between 50 and 100 °C. An Arrhenius expression of $k(T) = 16.8 \text{ s}^{-1} \exp(-16.6 \pm 0.7 \text{ kcal mol}^{-1}/RT)$ was obtained.

Table 2 Catalytic activity of 4Ti- β for cyclooctene epoxidation^a

Entry	Catalyst	Preparation route ^a	TON ^b	TOF ^c [h ⁻¹]	Ref.
1	Ti- β	Dealumination/impregnation	48	8	This work
2	Ti- β	Hydrothermal synthesis	20	10	18
3	Ti-MWW	Hydrothermal synthesis	147	73.5	18

^a Reaction conditions: 80 °C, 0.5 M in 2-butanol, olefin/H₂O₂ = 2, 1 mol% catalyst. ^b Defined as mole epoxide produced per mole Ti. ^c Mole epoxide produced per mole Ti per hour, over the entire time course of the reaction.

makes an overall assessment of its synthesis difficult, particularly since its activity for isomerisation reactions is predicted to be very low. Thus, to further verify the activity and nature of 4Ti- β , we also explored the epoxidation of bulky olefins by H₂O₂ with this catalyst. The epoxidation of olefins is a key reaction in the bulk and fine chemical industries, and when performed with H₂O₂, is a particularly green method for introducing functionality into key platform molecules. As can be seen (Table 2, ESI Fig. S2†), 4Ti- β demonstrates excellent catalytic activity for the epoxidation of cyclooctene, and is comparable in activity to other reported Ti- β catalysts prepared by more established preparation procedures, though it is still somewhat lower in activity than the current state of the art Ti-containing epoxidation zeolite (Ti-MWW).¹⁹ We note here that both Zr and Sn-containing β zeolites are known to be inactive for such epoxidation reactions.

Conclusions

A two-step procedure for the post-synthetic preparation of Lewis acidic Sn-, Zr- and Ti-zeolite β has been reported. Following dealumination of a parent aluminosilicate H- β zeolite, Lewis acidic centres can be incorporated into the vacant framework sites by solid-state ion-exchange (for Sn and Zr) or impregnation (Ti). The synthesised catalysts demonstrate excellent catalytic activity for the isomerisation of glyceraldehyde to dihydroxyacetone and/or the epoxidation of bulky olefins with H₂O₂. We believe that the ability to post-synthetically prepare such Lewis acidic zeolites from readily-available aluminosilicate analogues will lead to significant increases in the utilisation of these promising catalysts on an academic and industrial scale.

Experimental details

Commercial zeolite H- β (ZeoChem) was dealuminated by treatment in HNO₃ solution (13 M HNO₃, 100 °C, 20 h, 20 mL g⁻¹ zeolite). Solid-state ion-exchange was performed by grinding the appropriate amount of tin(II)acetate or zirconium(IV)ethoxide with the necessary amount of pre-dealuminated zeolite. Impregnation was performed by stirring dealuminated zeolite β in an ethanolic solution of titanium(IV)ethoxide. Following this procedure, the samples were heated in a combustion furnace to 550 °C for 3 h (20 °C min⁻¹ ramp rate) under a dry air flow.

FT-IR spectroscopy was performed on self-supporting wafers using a Bruker Alpha Spectrometer inside a glovebox in transmission mode. Intensities were normalized to the Si–O–Si overtones of the zeolite framework. DRUV-Vis analysis was performed with an Ocean Optics UV-Visible Spectrophotometer in diffuse reflectance mode. Si, Al, and other metal contents were determined by ICP-OES. Porosimetry measurements were performed on a Micromeritics Asap 2020 apparatus. The samples were degassed prior to use (275 °C, 3 h). Adsorption isotherms were obtained at 77 K and analyzed using BET and t-plot methods.

The isomerization of glyceraldehyde to dihydroxyacetone was carried out in a 50 mL round-bottomed flask equipped with a reflux condenser. The vessel was charged with the reactant solution (5 mL, 0.4 M glyceraldehyde in H₂O) and heated to the desired reaction temperature (50–100 °C). The reaction was initiated by adding the desired amount of catalyst (corresponding to a substrate/metal ratio of 100) and stirred vigorously for the required reaction period. Samples were taken periodically and quantified by HPLC.

The oxidation of cyclooctene was carried out in a 50 mL round-bottomed flask equipped with a reflux condenser. The vessel was charged with the reactant solution (10 mL, 0.5 M cyclooctene in 2-butanol) and heated to the desired reaction temperature (80 °C). The desired amount of catalyst was added to the vessel, and the reaction was subsequently initiated by adding the desired amount of H₂O₂ (0.5 M, H₂O₂/olefin = 1)

and stirred vigorously for the required reaction period. Samples were taken periodically and quantified by GC-FID against a biphenyl internal standard (30 m FFAP column).

Notes and references

- 1 A. Corma and H. Garcia, *Chem. Rev.*, 2003, **103**, 4307; Y. Román-Leshkov and M. E. Davis, *ACS Catal.*, 2011, **1**, 1566; A. Corma, *Catal. Rev. Sci. Eng.*, 2004, **46**, 369.
- 2 M. E. Domine and S. Valencia, *J. Catal.*, 2003, **215**, 294; A. Corma, F. X. Llabrés, I. Xamena, C. Prestipino, M. Renz and S. Valencia, *J. Phys. Chem. C*, 2009, **113**, 11306–11315.
- 3 A. Corma, L. T. Nemeth, M. Renz and S. Valencia, *Nature*, 2001, **412**, 423; M. Boronat, A. Comra, M. Renz, G. Sastre and P. M. Viruela, *Chem.–Eur. J.*, 2005, **11**, 6905; M. Renz, T. Blasco, A. Corma, V. Fornés, R. Jensen and L. Nemeth, *Chem.–Eur. J.*, 2002, **8**, 4708.
- 4 M. Moliner, Y. Román-Leshkov and M. E. Davis, *Proc. Natl. Acad. Sci. U. S. A.*, 2010, **107**, 6164; M. S. Holm, S. Saravanamurugan and E. Taarning, *Science*, 2010, **328**, 602; M. S. Holm, Y. J. Pagán-Torres, S. Saravanamurugan, A. Riisager, J. A. Dumesic and E. Taarning, *Green Chem.*, 2012, **14**, 702; A. Corma, M. E. Domine, L. Nemeth and S. Valencia, *J. Am. Chem. Soc.*, 2002, **124**, 3194.
- 5 J. M. R. Gallo, D. M. Alonso, M. A. Mellmer and J. Dumesic, *Green Chem.*, 2013, **15**, 85; E. Nikolla, Y. Román-Leshkov, M. Moliner and M. E. Davis, *ACS Catal.*, 2011, **1**, 408; E. Taarning, C. M. Osmundsen, X. Yang, B. Voss, S. I. Andersen and C. H. Christensen, *Energy Environ. Sci.*, 2011, **4**, 793.
- 6 P. Bai, J. I. Siepmann and M. W. Deem, *AIChE J.*, 2013, **59**, 3523.
- 7 L. Bui, H. Luo, W. R. Gunther and Y. Román-Leshkov, *Angew. Chem., Int. Ed.*, 2013, **52**, 1.
- 8 Y. Nie, S. Jaenicke and G.-K. Chuah, *Chem.–Eur. J.*, 2009, **15**, 1991.
- 9 Y. Kuwahara, D.-Y. Kang, J. R. Copeland, N. A. Brunelli, S. A. Didas, P. Bollini, C. Sievers, T. Kamegawa, H. Yamashita and C. W. Jones, *J. Am. Chem. Soc.*, 2012, **134**, 10757; Y. Kuwahara, D.-Y. Kang, J. R. Copeland, P. Bollini, C. Sievers, T. Kamegawa, H. Yamashita and C. W. Jones, *Chem.–Eur. J.*, 2012, **18**, 16649.
- 10 F. Cavani and J. H. Teles, *ChemSusChem*, 2009, **2**, 508; P. Wu, T. Tatsumi, T. Komatsu and T. Yashima, *J. Catal.*, 2001, **202**, 245; M. A. Camblor, M. Costantini, A. Corma, L. Gilbert, P. Esteve, A. Martinez and S. Valencia, *Chem. Commun.*, 1996, 1339.
- 11 Q. Guo, F. Fan, E. A. Pidko, W. N. P. van der Graaff, Z. Feng, C. Li and E. J. M. Hensen, *ChemSusChem*, 2013, **6**, 1352; C. Chang, Z. Wang, P. Dornath, H. J. Cho and W. Fan, *RSC Adv.*, 2012, **2**, 10475–10477; J. Dijkmans, D. Gabriëls, M. Dusselier, F. de Clippel, P. Vanelderen, K. Houthoofd, A. Malfliet, Y. Pontikes and B. F. Sels, *Green Chem.*, 2013, **15**, 2777–2785; P. Li, G. Liu, H. Wu, Y. Liu, J.-g. Jiang and P. Wu, *J. Phys. Chem. C*, 2011, **115**, 3663.
- 12 C. Hammond, S. Conrad and I. Hermans, *Angew. Chem., Int. Ed.*, 2012, **51**, 11736.
- 13 S. Dzwigaj, M. J. Peltre, P. Massiani, A. Davidson, M. Che, T. Sen and S. Sivasanker, *Chem. Commun.*, 1998, 87.
- 14 P. Wu, T. Komatsu and T. Yashima, *J. Phys. Chem.*, 1995, **99**, 10923.
- 15 P. Mania, R. Verel, F. Jenny, C. Hammond and I. Hermans, *Chem.–Eur. J.*, 2013, **19**, 9849; B. P. C. Hereijgers, R. F. Parton and B. M. Weckhuysen, *ACS Catal.*, 2011, **1**, 1183; T. Blasco, M. A. Camblor, A. Corma, P. Esteve, J. M. Guil, A. Martinez, J. A. Perdigon-Melon and S. Valencia, *J. Phys. Chem. B*, 1998, **102**, 75.
- 16 C. M. Osmundsen, M. S. Holm, S. Dahl and E. Taarning, *Proc. R. Soc. London, Ser. A*, 2012, **468**, 2000; S. Roy, K. Bakhmutsky, E. Mahmoud, R. F. Lobo and R. J. Gorte, *ACS Catal.*, 2013, **3**, 573; M. Boronat, P. Concepción, A. Corma, M. T. Navarro, M. Renz and S. Valencia, *Phys. Chem. Chem. Phys.*, 2009, **11**, 2876; M. Boronat, P. Concepción, A. Corma, M. Renz and S. Valencia, *J. Catal.*, 2005, **234**, 111.
- 17 Y. Román-Leshkov, M. Moliner, J. A. Labinger and M. E. Davis, *Angew. Chem., Int. Ed.*, 2010, **49**, 8954.
- 18 R. S. Assary and L. A. Curtiss, *J. Phys. Chem. A*, 2011, **115**, 2011.
- 19 P. Wu, D. Nuntasri, J. Ruan, Y. Liu, M. He, W. Fan, O. Terasaki and T. Tatsumi, *J. Phys. Chem. B*, 2004, **108**, 19126.